Neoplasia 63 (2025) 101159

Contents lists available at ScienceDirect

Neoplasia

journal homepage: www.elsevier.com/locate/neo

Original Research

MTFR1 phosphorylation-activated adaptive mitochondrial fusion is essential for colon cancer cell survival during glucose deprivation

Nan Zhang *, Lu Dong, Sifan Liu, Tingting Ning *, Shengtao Zhu *

Department of Gastroenterology, Beijing Friendship Hospital, Capital Medical University, State Key Laboratory for Digestive Health, National Clinical Research Center of Digestive Diseases, Beijing, 100050, China

ARTICLE INFO

Key words:
Colorectal cancer
Glucose deprivation
MTFR1
Mitochondrial fusion
NEK1

ABSTRACT

Background: Mitochondrial dynamics are essential for maintaining cellular function under metabolic stress. However, their role in colon cancer's response to glucose deprivation remains poorly understood.
Methods: The role of the mitochondrial protein MTFR1 in colon cancer proliferation was evaluated using CCK-8 and colony formation assays. Mass spectrometry identified MTFR1-interacting proteins and phosphorylation sites. Mitochondrial morphology was examined with Mitotracker staining, and mitochondrial function was evaluated using MitoSOX, JC-1 staining, and the Seahorse cell mitochondrial stress test.
Results: We observed that MTFR1 is highly expressed in colon cancer cells and interacts with NEK1 under glucose deprivation. This interaction induces phosphorylation of MTFR1 at serine 119, which promotes mitochondrial fusion and supports mitochondrial function. Consequently, enhanced oxidative phosphorylation improves cellular tolerance to glucose deprivation.
Conclusions: Our findings highlight the importance of MTFR1 in modulating mitochondrial dynamics and its potential impact on colon cancer cell survival under metabolic stress. These results suggest that MTFR1 serine 119 could be a key regulator of colon cancer cell metabolism and a potential therapeutic target for enhancing cancer cell response to metabolic challenges.

Introduction

Colorectal cancer (CRC) is a leading global malignancy, with 2 million new cases and about 1 million deaths reported in 2020 [1]. Despite advances in surgical treatments and combination chemotherapies, the 5-year survival rate for patients with advanced CRC remains low [2]. CRC cell survival under metabolic stress constitutes a pivotal stage not only for tumor growth but also for metastatic progression. Investigating their survival is essential for improving cancer therapies [3,4]. Glucose, a key energy source for cancer cells, plays a central role in their metabolism, and its deprivation represents a significant form of metabolic stress [5].

Mitochondria are essential for key biological processes such as energy metabolism, material metabolism, and signal transduction, which are critical for cell growth [6]. These organelles are highly dynamic, with mitochondrial fusion and fission playing central roles in regulating cellular metabolism in response to environmental changes [7]. However, the role of mitochondrial fusion in CRC cell adaptation to nutrient deprivation and its underlying mechanisms is not yet fully understood. Investigating how mitochondrial dynamics influence cellular metabolism and CRC proliferation will enhance our understanding of their involvement in colon cancer development.

Mitochondrial fission regulator 1 (MTFR1) is located on the mitochondrial inner membrane and regulates mitochondrial fission and fusion. In cardiomyocytes, MTFR1 knockdown inhibits mitochondrial fission, apoptosis, and exacerbates myocardial infarction [8]. In MTFR1-deficient testes, reduced mitochondrial oxygen consumption and ATP synthesis lead to oxidative DNA damage [9]. However, the role of MTFR1 in tumors remains unclear.

NEKs (Never in Mitosis A-related kinases) are a family of 11 protein kinases (NEK1-NEK11) homologous to the NIMA kinase from Aspergillus nidulans. These kinases play key roles in cell cycle regulation and are increasingly recognized for their involvement in the onset and progression of various cancers [10]. NEK1, in particular, has been implicated in colorectal cancer, glioblastoma, and clear cell renal cell carcinoma [11–13]. NEK1 is also involved in maintaining mitochondrial function [14], though its role in regulating mitochondrial dynamics in colorectal cancer has not been clarified.

* Corresponding authors.
E-mail addresses: zhangnan_2020@126.com (N. Zhang), ningtingting@mail.ccmu.edu.cn (T. Ning), zhushengtao@ccmu.edu.cn (S. Zhu).

https://doi.org/10.1016/j.neo.2025.101159
Received 10 February 2025; Received in revised form 12 March 2025; Accepted 13 March 2025

In this study, we found that MTFR1 is highly expressed in colon cancer cells. Under low-glucose conditions, MTFR1 interacts with NEK1, resulting in increased phosphorylation of serine 119, which promotes mitochondrial fusion and maintains mitochondrial function. This enhancement of oxidative phosphorylation improves the cells' tolerance to glucose deprivation. These findings highlight MTFR1′s role in regulating mitochondrial function in response to glucose availability, influencing colon cancer cell metabolism and survival under nutrient stress.

Methods

Cell culture

HCT116, SW480, HCT8, HT29, RKO, and NCM460 cells were cultured in high-glucose (4.5 g/L, Corning, 10-013-CV) or low-glucose (1 g/L, Corning, 10-014-CV) Dulbecco's modified Eagle medium (DMEM), supplemented with 10 % (vol/vol) fetal bovine serum (FBS) and appropriate penicillin/streptomycin concentrations. Cultures were maintained in an incubator at 37 °C with 5 % CO_2.

Plasmid constructions

The plasmids flag-MTFR1, flag-MTFR1-S119A, and flag-MTFR1-S119D were purchased from Youbao Bio (Shanghai, China). The plasmids used for CRISPR-Cas9 gene editing were pSpCas9(BB)-2APuro (PX459, Addgene ID 48139). The sequences of the sgRNA oligos used for gene targeting were: MTFR1-1: 5′-GATTA AGCGC CTAAT TAGGA-3′; MTFR1-2: 5′-GTGGC GTCTT TTGCT GATGT-3′. shRNA sequences as used in this study are as follows: shNEK1:5′-ACAAA GCCTG CCGCT AAATA T-3′. shRNA oligonucleotides were purchased from Shanghai GenePharma Company. These plasmids were transfected into cells using the Lipofectamine 2000 transfection kit (Invitrogen) according to the manufacturer's instructions.

RNA extraction and quantitative real-time PCR

Total RNA was extracted from two cell lines using TRIzol (Invitrogen) according to the manufacturer's protocol. Random primers were used for reverse transcription. Quantitative PCR was performed using SYBR-Green mix (Invitrogen) and run in a 7500 Real-Time PCR System (Applied Biosystems) with the following cycling parameters: 94 °C for 2 min; 40 cycles of 94 °C for 15 s, 56 °C for 20 s and 72 °C for 30 s; and 72 °C for 2 min. With a melting curve analysis, ΔΔCT analysis was applied to determine qPCR results. Each analysis was performed in triplicate. The qPCR primer sequences are:

β-actin: CCAACCGCGAGAAGATGA, CCAGAGGCGTACAGGGATAG;
MTFR1: ATGTTGGATGGGTAGCCAAAG, TTCGAGAGCGCAAATCT TCTG;
NEK1: AATGCTCAGAAAGGCGTTTTGT, GGGGTCCCTATGCAAGT TCG.

Antibodies

The antibodies used were anti-β-actin (Santa Cruz, sc-7210), anti-vinculin (Abcam, ab207440), anti-flag-tag (Sigma-Aldrich, F1804), anti-MTFR1 (Proteintech, 17778-1-AP), anti-Phospho-(Ser/Thr) Phe (CST, 9631), anti-NEK1 (Proteintech, 27146-1-AP), and anti-Noxa (Santa Cruz, sc-56169).

Western blotting

Equal amounts of proteins (20–50 μg) were size fractionated by 6–15 % SDS polyacrylamide gel electrophoresis.

Co-immunoprecipitation (CO-IP)

Cells were harvested and then lysed in lysis buffer (0.5 % NP-40, 150 mM NaCl, 50 mM Tris at pH 7.5, 5 mM EDTA, and 1 % EDTA-free protease and phosphatase inhibitor cocktails (Roche Applied Science) on ice for 25 min. After centrifugation at 4 °C at 12,000 rpm for 15 min, 2 μg of the indicated antibody was added into the supernatant and incubated at 4 °C overnight. Then, 30 μl of Protein A + G Agarose (Beyotime Biotechnology) was added and incubated for 2 h at 4 °C. The beads were washed with NP-40 buffer three times. The precipitated components were analyzed by western blotting.

Cell viability

Changed cell viability was assayed using a cell counting kit-8 (CCK-8) kit (Beyotime Biotechnology, C0039). In brief, HCT116 and HCT8 cells were grown in 96-well plates at a density of 2×10^3 cells/well. At the end of each experiment, cell culture was added with the CCK-8 reagent, and cells were further cultured for 1 h and the optical density of cell culture was then measured at 450 nm. Cell viability was determined in terms of the proportion of cell survival, compared with control.

Colony formation assay

Cells were plated at the indicated densities onto 6-well plates. 24 h after plating, cells were washed twice with PBS and incubated in high- or low- glucose DMEM for 48 h, which was followed by a recovery period in normal growth medium. After the recovery period, cells were washed with PBS, and stained using 0.5 % crystal violet. The colony area was determined by using the Colony Area plugin and ImageJ software.

Mitochondrial morphology

To assess mitochondrial morphology, cells were seeded into confocal dishes and cultured with Mito-Tracker Red probe (Beyotime, C1035) for 30 min at 37 °C. They were then washed using PBS three times for analysis using an Olympus Microscope (Olympus, Japan). Mitochondrial length was measured using ImageJ-Mitochondria Analyzer plugins (https://github.com/AhsenChaudhry/Mitochondria-Analyzer). >50 cells were analyzed per sample.

Quantification of mitochondrial superoxide levels

Cells were treated with 1 μM mitoSOX red (MCE, HY-D1055) for 30 min at 37 °C. Then trypsinized the cells and measured fluorescence using flow cytometry.

Mitochondrial membrane potential assay

The mitochondrial membrane potential was assessed using the JC-1 Assay Kit (Beyotime, C2003S), and images were subsequently captured using a confocal microscope.

DNA isolation and mitochondrial DNA (mtDNA) copy number analysis

HCT116 cells were harvested and divided into two equal aliquots. One aliquot was retained for intact cells, while the other was processed using the Mitochondria Isolation Kit (Beyotime, C3601) according to the manufacturer's protocol to obtain the cytosolic fraction. DNA was extracted from both fractions using the Tiangen Micro Sample Genomic DNA Extraction Kit (Tiangen, DP316). A total of 10 ng of DNA from each fraction was subjected to real-time PCR. The copy number of cytosolic mtDNA was normalized to that of whole-cell nuclear DNA by calculating the ratio of mtDNA encoding cytochrome c oxidase I (primers: 5′- GCCCC CGATA TGGCG TTT -3′ and 5′- GTTCA ACCTG TTCCT GCTCC -3′) to nuclear DNA encoding 18S rDNA (primers: 5′- TAGAG GGACA AGTGG

CGTTC -3′ and 5′- CGCTG AGCCA GTCAG TGT -3′).

Measurement of ATP levels

Cells were collected, boiled in water and then lysed ultrasonically. The intracellular ATP content was quantified using the ATP Assay Kit (Nanjing Jiancheng, A095-1-1).

Seahorse XF cell mito stress test

The oxygen consumption rate (OCR) was measured by an XF extracellular analyzer (Agilent Technologies). HCT116 were seeded at 2×10^4 cells/well density in 24-well plates for overnight incubation to allow adherence to the plate. Then the cells were cultured in low-glucose medium for 24 h. The cells replaced to Seahorse XF assay Medium (Agilent) pH 7.4 supplemented with 10 mM glucose, 1 mM pyruvate, and 2 μM glutamine. After monitoring of basal respiration, sequential injection 1.5 μM of mitochondrial inhibitors oligomycin, 1 μM FCCP, and 0.5 μM Rotenone/antimycin A provided by the manufacturer (Agilent, 101706–100). OCR was automatically calculated using the Seahorse XF software. Every point represents an average of three different wells.

Immunohistochemical (IHC) staining

The colon cancer tissue microarray was purchased from Shanghai OUTDO Biotechnology (OD-CT-DgCol04-001). For IHC analysis, 3 mm sample sections were incubated with anti-MTFR1-S119ph (1:100), and anti-NEK1 (1:50) respectively, overnight at 4 °C in a humidified chamber, followed by incubation with the HRP-conjugated secondary antibodies for 2 h. Staining was completed by 5–10 min incubation with diaminobenzidine (DAB) substrate, which resulted in a brown-colored precipitate at the antigen site.

Nude mice tumor xenograft

All mice used in this study were supplied by and housed under specific pathogen-free conditions at Capital Medical University (Beijing, China). Six-week-old male BALB/c nude mice were used for tumorigenesis and the mice were randomly divided into 2 groups ($n = 6$). 5×10^6 treated HCT116 cells were injected subcutaneously into mice. When tumors were approximately 200 mm^3 in size, the animals were received 0.2 ml of 2-Deoxy-D-glucose (Selleck, S4701) i.p. at 75 mg/ml (500 mg/kg), which was repeated 3 times per week for the duration of the experiment. 6 weeks after inoculation, the mice were killed, the tumors were weighed, and the volume was measured by using the formula $0.52 \times L \times W^2$. All experiments were performed according to Animal Utilization Protocols and reviewed by the Animal Experiments and Experimental Animal Welfare Committee of Capital Medical University.

Statistical analysis

Data are shown as the mean ± SD for the experiments repeated with at least 3 replicates. The sample size was generally chosen based on preliminary data indicating the variance within each group and the differences between groups. All statistical analyses were performed using GraphPad Prism 9.4.1. Significance of the difference between two groups was determined using unpaired Student's t-tests after accounting for equality of variances using an F test. n.s. $p > 0.05$, $*p < 0.05$, $**p < 0.01$.

Results

MTFR1 is overexpressed in colon cancer and plays critical roles in regulating cell proliferation and survival

Previous studies have shown that energy stress induces mitochondrial elongation in tumor cells [15]. We cultured colon cancer cell lines HCT116 and HCT8 in high-glucose and low-glucose media for 24 hours, followed by Mitotracker staining to assess mitochondrial length. The results demonstrated that glucose deprivation triggers mitochondrial fusion in these cells (Fig. 1A).

To explore the molecular mechanisms underlying mitochondrial fusion in colon cancer, we analyzed TCGA mRNA expression data for genes involved in mitochondrial dynamics. Notably, MTFR1 expression levels were significantly different between normal and colon cancer tissues (Figure S1A). We also analyzed mRNA expression data from GEO database to assess MTFR1 expression in colon cancer. As can be seen in Fig. 1B, MTFR1 expression was dramatically upregulated in colon cancer tissues compared to adjacent normal tissues across four independent GEO datasets (GSE8671, GSE20916, GSE41258, and GSE110224).

Moreover, MTFR1 mRNA and protein levels were measured in five colon cancer cell lines (SW480, HCT116, HCT8, HT29, and RKO) and human normal colorectal epithelial cell line NCM460. MTFR1 expression was notably higher in colon cancer cell lines, particularly in HCT116 and HCT8, compared to NCM460 (Fig. 1C and 1D).

To elucidate the function of MTFR1 in colon cancer, we generated MTFR1-knockout (MTFR1-KO) HCT116 and HCT8 cell lines using CRISPR-Cas9, with knockout confirmed by western blotting (Fig. 1E). We then assessed the impact of MTFR1 on cell viability through CCK-8 (Fig. 1F) and colony formation assays (Fig. 1G). Compared to wild-type (WT) cells, MTFR1-KO cells showed a slight reduction in proliferation. However, under low-glucose conditions, MTFR1-KO cells exhibited enhanced survival. These findings suggest that MTFR1 regulates the survival of colon cancer cells under low-glucose conditions.

Low glucose induces MTFR1 phosphorylation in colon cancer cells

We next investigated the mechanisms underlying the differential role of MTFR1 in regulating colon cancer cell proliferation under low- and high-glucose conditions. Colon cancer cell lines HCT116 and HCT8 were cultured in both high-glucose and low-glucose media, and MTFR1 mRNA and protein levels were analyzed. No significant differences were observed (Fig. 2A and 2B). Since protein phosphorylation plays a critical role in regulating protein function [16], we next assessed MTFR1 phosphorylation via IP using an anti-MTFR1 antibody, followed by immunoblotting with an anti-phospho-(Ser/Thr) antibody. The results demonstrated elevated MTFR1 phosphorylation under low-glucose conditions compared to high-glucose conditions (Fig. 2C).

NEK1 catalyzes the phosphorylation of MTFR1

We focused on potential mechanisms underlying MTFR1 phosphorylation. A mass spectrometry analysis was performed to identify endogenous proteins associated with flag-tagged MTFR1 in HCT116 cells. MTFR1 immunoprecipitated contained NEK1, a kinase frequently dysregulated in cancer [10]. The interaction between MTFR1 and NEK1 was confirmed in transfected HCT116 cells using epitope-tagged constructs (Fig. 3A). Additionally, the endogenous MTFR1-NEK1 complex was detected by co-IP analysis in colon cancer cells (Fig. 3B).

To further validate the involvement of NEK1 in regulating MTFR1 phosphorylation levels, we employed shRNA to knock down NEK1 expression (Fig. 3C). Consequently, MTFR1 phosphorylation was detected by IP using an anti-MTFR1 antibody, followed by immunoblotting with an anti-phospho-(Ser/Thr) antibody. We observed a reduction in MTFR1 phosphorylation levels upon NEK1 knockdown (NEK1-KD) (Fig. 3D). Additionally, HCT116 cells were cultured under

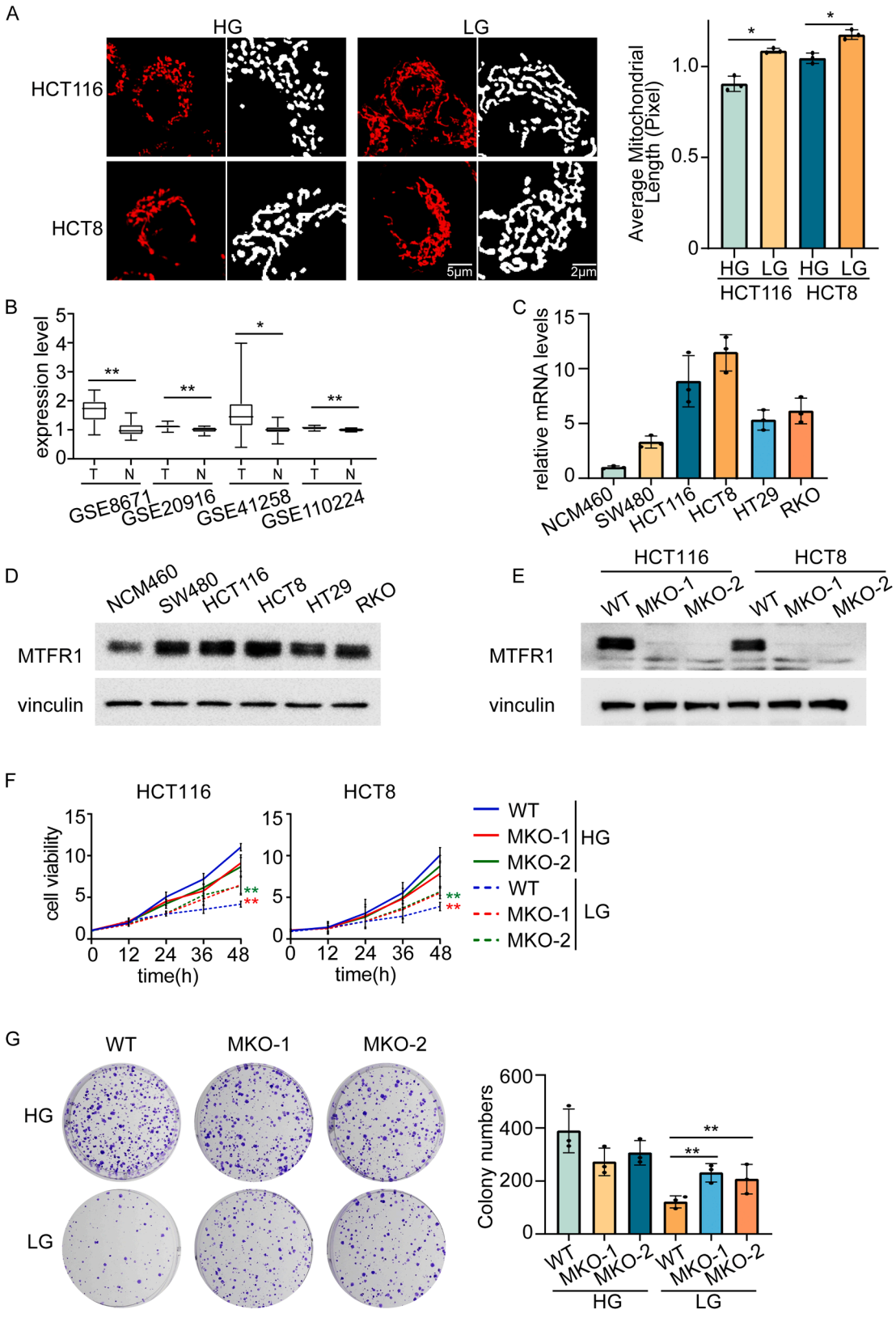

Fig. 1. MTFR1 is elevated in colon cancer and regulates cell survival.

A. CRC cells were cultured in high- or low-glucose DMEM for 24h. Representative confocal images of mitochondrial morphology were shown. Right, the average mitochondrial length was quantified. B. Variation in MTFR1 mRNA expression level between normal tissues (N) and CRC (T) based on GEO data sets (GSE8671, GSE20916, GSE41258, and GSE110224). C. MTFR1 mRNA expression levels in CRC cells and normal colonic NCM460 cells. D. MTFR1 protein levels in CRC cells and NCM460 were measured using western blotting. E. Western blotting was performed to determine MTFR1 protein levels. F. WT and MTFR1-KO CRC cells were cultured in low-glucose DMEM for the indicated times. Cell viability was then tested with the CCK-8 assay. Data are shown as mean ± SD ($n = 3$). G. WT and MTFR1-

KO HCT116 cells were cultured in high- or low-glucose DMEM, and a clonogenic survival assay was performed. Colonies were counted after crystal violet staining, and the quantitative data are shown as the mean ± SD ($n = 3$).

low-glucose conditions, and co-IP experiments demonstrated that, while low glucose did not alter NEK1 protein expression, it significantly enhanced the interaction between NEK1 and MTFR1 (Fig. 3E).

Serine 119 is the phosphorylation site in MTFR1

Mass spectrometry identified serine 119 (S119) as a phosphorylation site on MTFR1 (Fig. 4A). To verify if S119 is a phosphorylation site of MTFR1 in colon cancer, we constructed a simulated dephosphorylation mimic plasmid, MTFR1-S119A. WT and mutant (S119A) MTFR1 plasmids were overexpressed in HCT116 cells, and their phosphorylation status was assessed by IP using anti-flag antibody, followed by immunoblotting for anti-phospho-(Ser/Thr) antibody. As shown in Fig. 4B, MTFR1-WT could be phosphorylated, whereas MTFR1-S119A remained unphosphorylated.

We next generated a specific antibody to detect MTFR1-S119 phosphorylation. As expected, MTFR1-S119 phosphorylation levels increased under low-glucose conditions (Fig. 4C). To further confirm that MTFR1-S119 is phosphorylated by NEK1, we measured its phosphorylation levels in NEK1-KD cells. In these cells, MTFR1-S119 phosphorylation was significantly reduced (Fig. 4D), indicating that NEK1 is crucial for regulating phosphorylation at this site.

We overexpressed MTFR1-WT and MTFR1-S119A in MTFR1-KO cells and used siRNA to suppress NEK1 expression to examine MTFR1 phosphorylation levels. As expected, NEK1 inhibition resulted in a decrease in MTFR1-WT phosphorylation. However, MTFR1-S119A phosphorylation levels was unaffected by NEK1 suppression (Fig. 4E), confirming that NEK1 specifically phosphorylates MTFR1 at S119.

We also conducted IHC to assess NEK1 expression and MTFR1-S119 phosphorylation levels in colon cancer tissues from patients. Notably, we observed a positive correlation between NEK1 and MTFR1-S119ph, suggesting an association between these two proteins in colon cancer (Fig. 4F).

NEK1 regulates mitochondrial fusion by phosphorylating MTFR1

We next investigated whether MTFR1-S119 phosphorylation affects mitochondrial fusion. In MTFR1-KO cells, we performed overexpression experiments with an empty vector, MTFR1-WT, non-phosphorylatable MTFR1-S119A, and phosphomimetic MTFR1-S119D. Using confocal microscopy to assess mitochondrial morphology, we observed that mitochondria in MTFR1-S119D cells were significantly longer compared to those in MTFR1-S119A cells (Fig. 5A), indicating that MTFR1-S119 phosphorylation promotes mitochondrial fusion.

To elucidate the involvement of NEK1 in regulating mitochondrial fusion, we employed confocal microscopy to observe mitochondrial morphology in NEK1-KD colon cancer cells. Our results demonstrated that NEK1 knockdown reduced mitochondrial length, suggesting that NEK1 is crucial for maintaining the balance between mitochondrial fusion and fission (Fig. 5B). To further confirm that NEK1 regulates mitochondrial fusion via MTFR1-S119 phosphorylation, we overexpressed MTFR1-WT and MTFR1-S119D in MTFR1-KO cells and used siRNA to suppress NEK1 expression. As can be seen in Fig. 5C, inhibiting NEK1 in WT-expressing cells led to a reduction in mitochondrial length, indicating that NEK1 kinase activity is involved in preventing mitochondrial elongation. However, when NEK1 was inhibited in MTFR1-S119D-expressing cells, no significant changes in mitochondrial morphology were observed. This suggests that the phosphomimetic MTFR1-S119D mutant can bypass NEK1′s regulatory effect on mitochondrial dynamics, further supporting the idea that S119

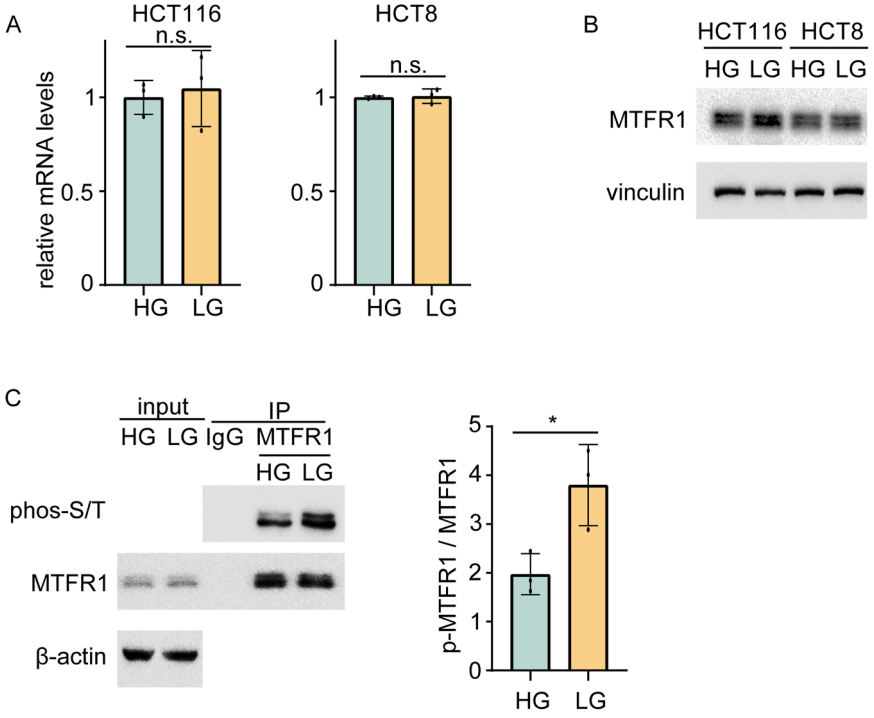

Fig. 2. Low glucose triggers MTFR1 phosphorylation.
A. CRC cells were cultured in high- or low-glucose DMEM for 24h. MTFR1 mRNA levels were analyzed with real-time PCR. Data are shown as mean ± SD ($n = 3$). B. CRC cells were cultured in high- or low-glucose DMEM for 24h. MTFR1 protein levels were analyzed with western blotting. C. HCT116 cells were cultured in high- or low-glucose DMEM for 24h. Proteins were IP with an antibody to MTFR1 followed by IB with an antibody to phosphorylated-serine/ threonine. Right, quantitative analysis results of phos-S/T ($n = 3$).

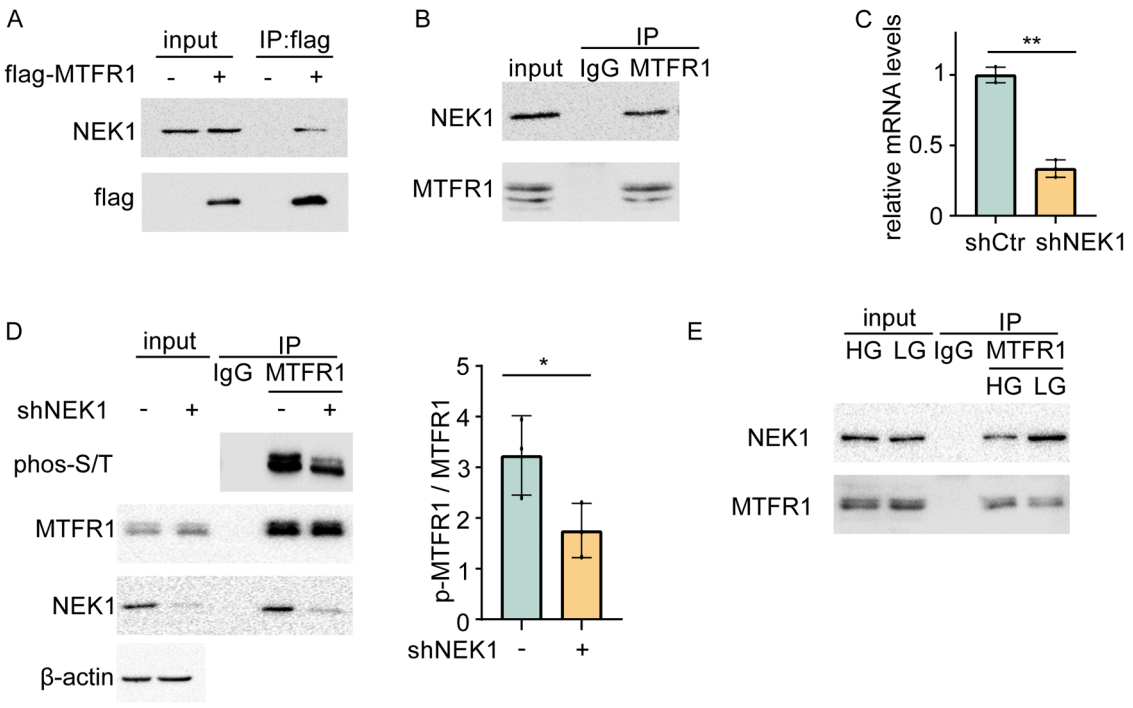

Fig. 3. NEK1 phosphorylates MTFR1.
A. HCT116 cells were transfected with an empty vector or flag-MTFR1 plasmids. 24h after transfection, the cell lysate was extracted for co-IP with anti-flag antibody. B. HCT116 cell lysates were extracted for co-IP using anti-MTFR1 antibody. C. QPCR was performed to determine NEK1 mRNA levels. Data are shown as mean ± SD ($n = 3$). D. WT and NEK1-KD HCT116 cell lysates were extracted for co-IP using anti-MTFR1 antibody. Right, quantitative analysis results of phos-S/T ($n = 3$). E. HCT116 cells were cultured in high- or low-glucose DMEM for 24h, the cell lysate was extracted for co-IP with anti-MTFR1 antibody.

phosphorylation is a key target of NEK1 in modulating mitochondrial fusion.

MTFR1 phosphorylation-mediated mitochondrial fusion alleviates mitochondrial dysfunction under glucose deprivation

Under energetic stress, mitochondrial respiration byproducts, particularly reactive oxygen species (ROS), accumulate alongside damaged mitochondria, leading to cell death [17]. To evaluate the impact of MTFR1 on mitochondrial function in CRC cells, we measured mitochondrial superoxide levels using MitoSOX Red, a specific probe for mitochondrial ROS. Flow cytometry analysis revealed significantly lower mitochondrial ROS levels in S119D cells compared to S119A cells (Fig. 6A), indicated that S119D reduces mitochondrial superoxide accumulation. We next evaluated mitochondrial membrane potential using JC-1, a probe that fluoresces red when accumulating in healthy mitochondria but emits green fluorescence when released from damaged mitochondria into the cytoplasm. Fluorescence microscopy showed higher red fluorescence in S119D cells compared to S119A cells (Fig. 6B).

To assess mitochondrial damage, we measured mtDNA levels in the cytoplasm. Under low-glucose conditions, S119A cells exhibited higher mtDNA levels in the cytoplasm compared to S119D cells, suggesting greater mitochondrial damage in S119A cells (Fig. 6C). Additionally, we examined Noxa, a pro-apoptotic protein associated with mitochondrial damage. After overexpressing vector, MTFR1-WT, MTFR1-S119A, and MTFR1-S119D in MTFR1-KO cells, we subjected them to low-glucose treatment and measured Noxa protein levels. The results showed significantly lower Noxa levels in MTFR1-S119D cells compared to MTFR1-S119A cells, indicating that S119A cells experienced more severe mitochondrial damage under low-glucose conditions (Fig. 6D).

Together, these findings suggest that MTFR1-S119 phosphorylation mitigates mitochondrial dysfunction induced by glucose deprivation.

MTFR1-S119 phosphorylation-mediated fusion enhances oxidative phosphorylation

Numerous investigations have shown that mitochondrial fusion in response to energy stress plays a regulatory role in glucose metabolism [18]. Under low-glucose conditions, cancer cells may rely more on oxidative phosphorylation to efficiently produce ATP [19].

We first measured ATP levels in MTFR1-KO cells under glucose deprivation and found that ATP levels were higher in S119D cells compared to S119A cells (Fig. 7A). Metabolic profiling of HCT116 cells subjected to starvation, using the Seahorse Flux Analyzer, revealed a higher oxidative phosphorylation rate in S119D cells than in S119A cells (Fig. 7B). These results suggest that MTFR1 phosphorylation at residue 119 promotes fusion, thereby enhancing oxidative phosphorylation in colon cancer cells under low-glucose conditions.

MTFR1 phosphorylation is crucial for colon cancer cell survival under glucose deprivation

To investigate the role of MTFR1-mediated mitochondrial fusion in tumor cell survival under glucose deprivation, we performed CCK-8 and colony formation assays in HCT116 and HCT8 cells under starvation conditions. MTFR1-KO cells transfected with MTFR1-S119A, when exposed to low-glucose conditions, showed a significant reduction in cell proliferation (Fig. 8A and 8B), indicating that MTFR1-S119 phosphorylation-mediated mitochondrial fusion plays a protective role in colon cancer cells during glucose starvation.

To explore the impact of MTFR1-S119D-mediated mitochondrial fusion on tumor growth in vivo, we overexpressed MTFR1-S119A or MTFR1-S119D in MTFR1-KO HCT116 cells and established a xenograft nude mouse model. To simulate a glucose-deprived environment, the mice were treated with the glucose analogue 2-deoxy-D-glucose (2-DG). Compared to the S119A-expressing cells, the S119D-expressing cells demonstrated significantly enhanced proliferative capacity (Fig. 8C-E).

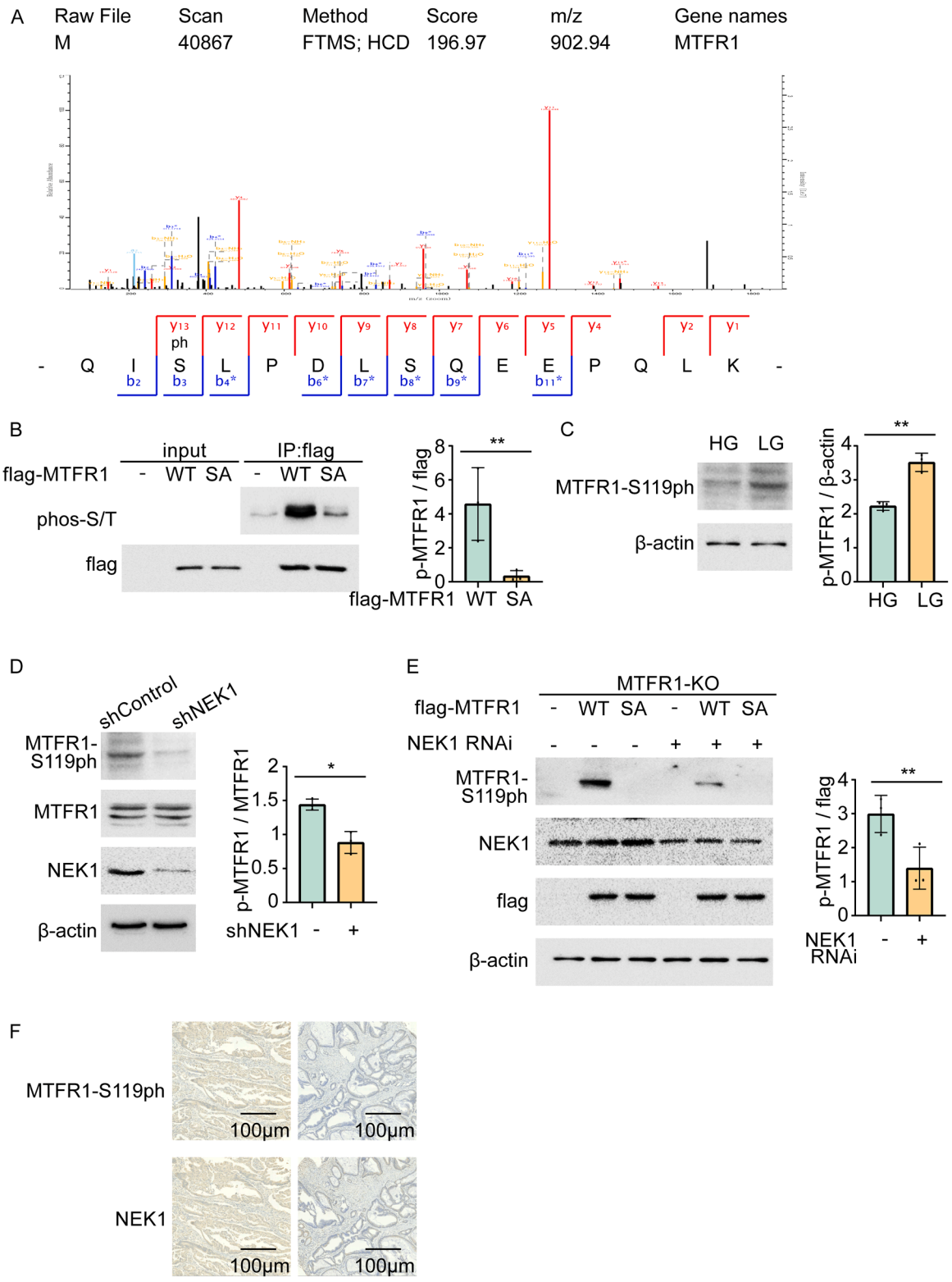

Fig. 4. Phosphorylation of Serine 119 in MTFR1 by NEK1.
A. Identification of S119 phosphorylation on MTFR1 by using mass spectrometry analysis. B. MTFR1-KO HCT116 cells were transfected with flag-MTFR1-WT or flag-MTFR1-S119A plasmid, 24h post-transfection, cells were cultured in low-glucose DMEM for 24h, the cell lysate was extracted for IP with an antibody to flag followed by IB with an antibody to phosphorylated-serine/ threonine. Right, quantitative analysis results of phos-S/T ($n = 3$). C. HCT116 cells were cultured in high- or low-glucose DMEM for 24h. MTFR1 phosphorylation levels were analyzed with western blotting. Right, quantitative analysis results of MTFR1-S119ph ($n = 3$). D. WT and NEK1-KD HCT116 cell lysates were extracted to detect MTFR1 phosphorylation levels with western blotting. Right, quantitative analysis results of MTFR1-S119ph ($n = 3$). E. MTFR1-KO HCT116 cells were transfected with flag-MTFR1-WT or flag-MTFR1-S119A plasmid, 24h post-transfection, cells were cultured in low-glucose DMEM for 24h, the cell lysate was extracted to detect MTFR1 phosphorylation levels with western blotting. Right, quantitative analysis results of MTFR1-S119ph ($n = 3$). F. Immunohistochemical staining of MTFR1-S119ph and NEK1 in colorectal cancer tissues.

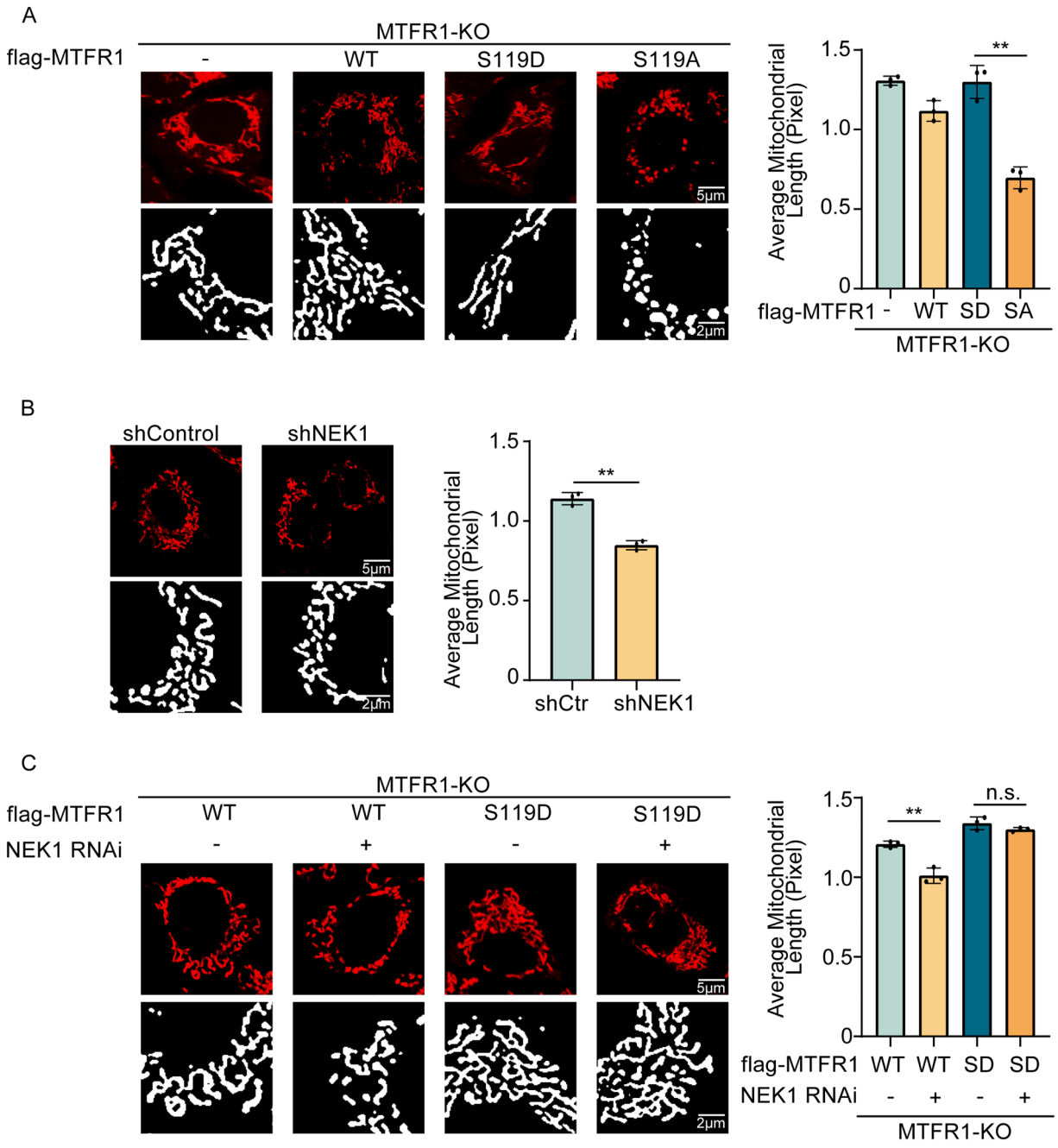

Fig. 5. NEK1 controls mitochondrial fusion through MTFR1 phosphorylation.
A. MTFR1-KO HCT8 cells were transfected with flag-MTFR1-WT, flag-MTFR1-S119D, or flag-MTFR1-S119A plasmid, 24h post-transfection, cells were cultured in low-glucose DMEM for 24h. Representative confocal images of mitochondrial morphology were shown. Right, the average mitochondrial length was quantified. B. Representative confocal images of mitochondrial morphology of WT and NEK1-KD HCT8 cells were shown. Right, the average mitochondrial length was quantified. C. MTFR1-KO HCT8 cells were transfected with NEK1 siRNA and flag-MTFR1-WT or flag-MTFR1-S119D plasmid, 24h post-transfection, cells were cultured in low-glucose DMEM for 24h. Representative confocal images of mitochondrial morphology were shown. Right, the average mitochondrial length was quantified.

These findings suggest that MTFR1-S119 phosphorylation is essential for colon cancer cells survival under low-glucose conditions.

Discussion

The tumor microenvironment is typically characterized by diminished glucose availability owing to rapid cell growth and inadequate blood circulation [20]. Insufficient glucose can impede cell growth by diminishing energy and metabolite levels [21]. Consequently, cancer cells undergo adaptive responses, including the activation of signaling pathways and metabolic reprogramming, to survive under such constrained conditions [22]. Investigating how tumors adapt to glucose-deficient environments is pivotal for comprehending tumor progression.

Mitochondrial fusion is crucial for maintaining mitochondrial function in tumors under metabolic stress. Studies have demonstrated that various mechanisms regulate mitochondrial fusion to support cell survival by preserving mitochondrial integrity under metabolic stress, including dynamin-related protein 1 (Drp1) phosphorylation [15,18, 23–25], mitofusin 1 (MFN1) deacetylation [26], and ubiquitin-like protein 4A- actin-related protein 2/3 (Ubl4A-Arp2/3) interactions [27]. Additionally, research indicates that the mitochondrial fusion

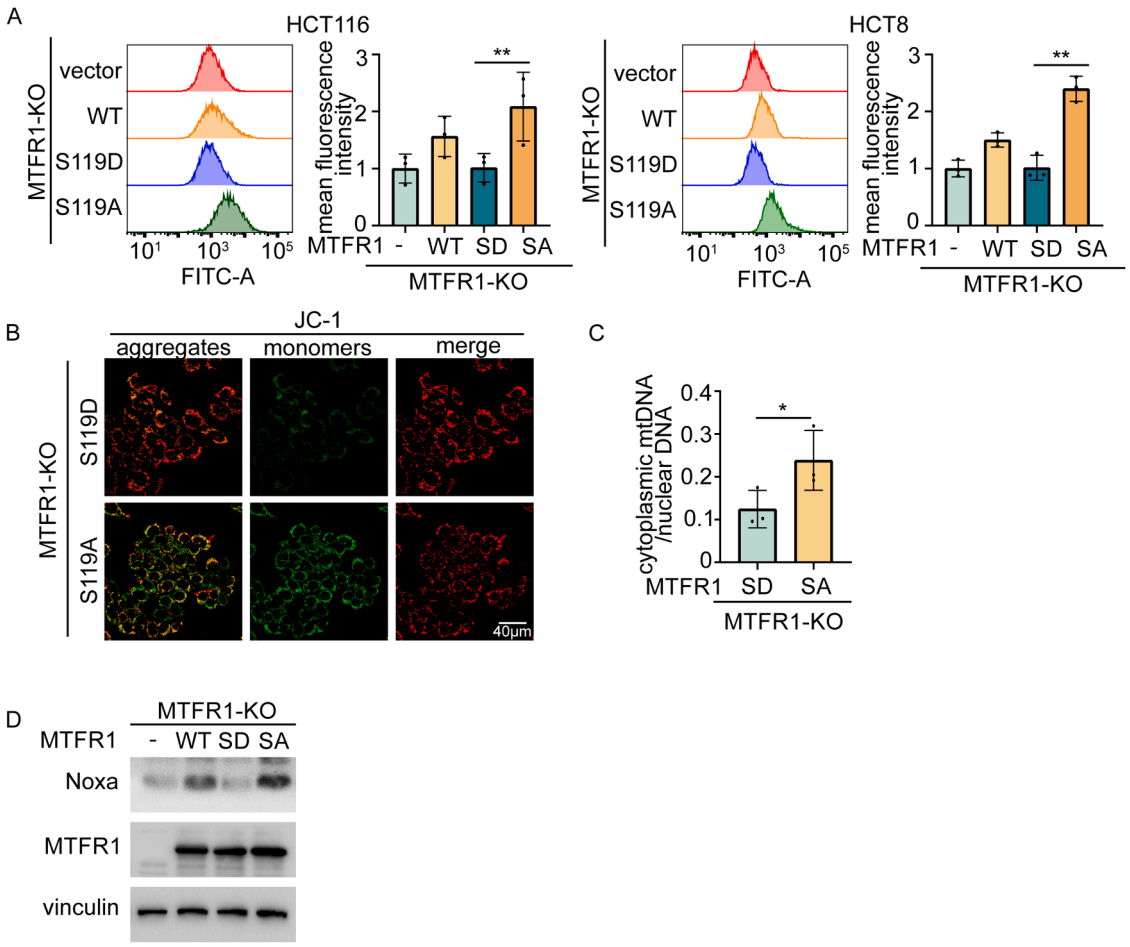

Fig. 6. MTFR1 phosphorylation-induced mitochondrial fusion maintains mitochondrial function.
A. MTFR1-KO CRC cells were transfected with flag-MTFR1-WT, flag-MTFR1-S119D, or flag-MTFR1-S119A plasmid, 24h post-transfection, cells were cultured in low-glucose DMEM for 24h, stained with MitoSOX, and analyzed by flow cytometry. Representative flow cytometry histogram and mean fluorescence intensity were shown. B. JC-1 staining of MTFR1-KO HCT116 cells expressing flag-MTFR1-S119D or MTFR1-S119A, cultured in low-glucose DMEM for 24h, to assess mitochondrial membrane potential. C. QPCR analysis of mtDNA release in MTFR1-KO HCT116 cells expressing flag-MTFR1-S119D or MTFR1-S119A, cultured in low-glucose DMEM for 24h. Data are shown as mean ± SD (n = 3). D. MTFR1-KO CRC cells were transfected with flag-MTFR1-WT, flag-MTFR1-S119D, or flag-MTFR1-S119A plasmid, 24h post-transfection, cells were cultured in low-glucose DMEM for 24h. Noxa protein levels were analyzed with western blotting.

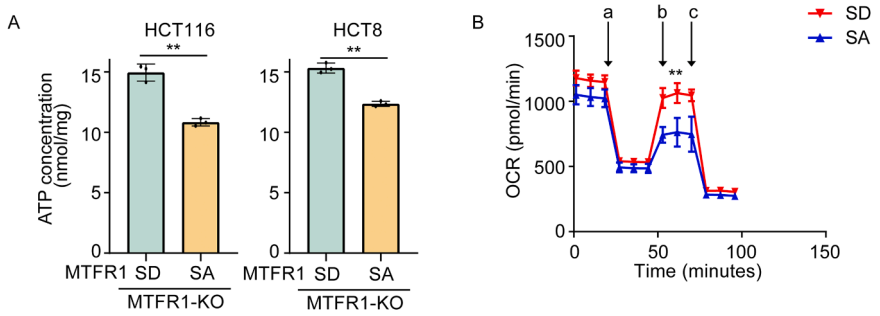

Fig. 7. MTFR1-S119 phosphorylation-driven fusion boosts oxidative phosphorylation.
A. ATP concentration in MTFR1-KO HCT116 cells expressing flag-MTFR1-S119D or MTFR1-S119A, cultured in low-glucose DMEM for 24h. Data are shown as mean ± SD (n = 3). B. Mitochondrial respiration reflected by OCR levels was detected in HCT116 cells expressing flag-MTFR1-S119D or MTFR1-S119A, cultured in low-glucose DMEM for 24h (a, 1.5μM oligomycin, b, 1μM FCCP, c, 0.5μM Rotenone/antimycin A). Data are shown as mean ± SD (n = 4).

machinery regulates energy deprivation-induced autophagy by sustaining mitochondrial respiration [28], highlighting its critical role in tumor cell adaptation to nutrient-deficient environments. Our study found that MTFR1 regulates mitochondrial fusion in colon cancer cells under low-glucose conditions, suggesting that it may serve as a key mitochondrial molecule in response to energy stress.

The MTFR1 family includes three members: MTFR1, MTFR1L, and MTFR2. AMPK-mediated phosphorylation of MTFR1L has been shown to induce mitochondrial elongation and promote fusion events, a process facilitated by increased levels of the fusion protein optic atrophy 1 [29]. Our mass spectrometry data did not detect any interaction between AMPK and MTFR1. Further research is needed to determine whether a

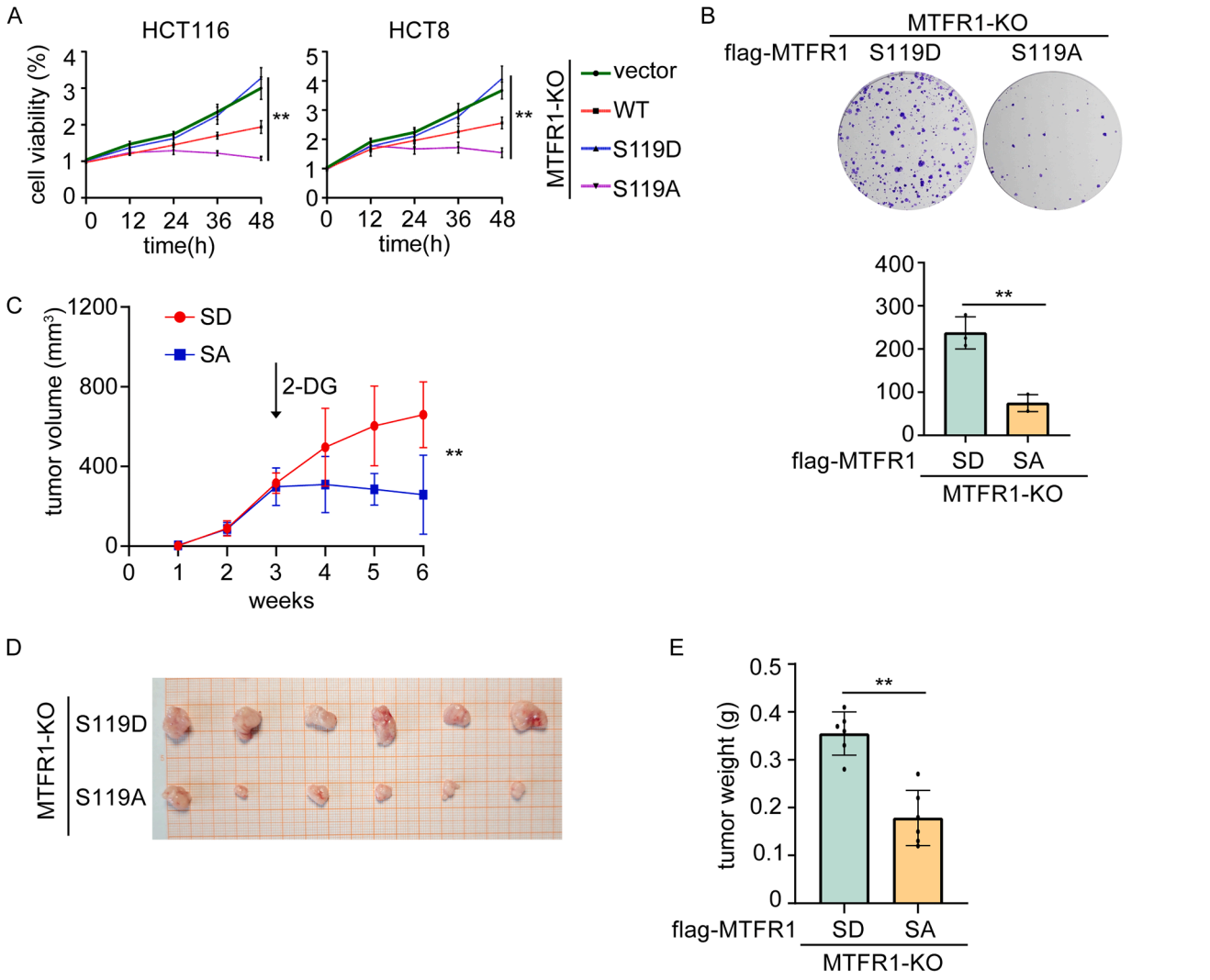

Fig. 8. MTFR1 phosphorylation is vital for colon cancer cell survival.
A. MTFR1-KO CRC cells expressing flag-MTFR1-WT, flag-MTFR1-S119D, or flag-MTFR1-S119A were cultured in low-glucose DMEM for the indicated times. Cell viability was then tested with the CCK-8 assay. Data are shown as mean ± SD ($n = 3$). B. MTFR1-KO HCT116 cells expressing flag-MTFR1-S119D or MTFR1-S119A were cultured in low-glucose DMEM, and a clonogenic survival assay was performed. Colonies were counted after crystal violet staining, and the quantitative data are shown as the mean ± SD ($n = 3$). C. MTFR1-KO HCT116 cells expressing flag-MTFR1-S119D or MTFR1-S119A were injected into BALB/c nude mice, and tumor growth was monitored ($n = 6$). D-E. Xenograft weight and size were measured ($n = 6$).

similar regulatory mechanism exists. Additionally, MTFR2-dependent mitochondrial fission has been linked to the progression of hepatocellular carcinoma [30] and oral squamous carcinoma [31], but its role in colorectal cancer development and progression remains to be explored.

NEK1 is a member of a highly conserved family of serine/threonine kinases that play key roles in cell cycle regulation, ciliogenesis, and the DNA damage response [32–35]. Under basal conditions in dividing cells, NEK1 is predominantly localized to the centrosome at the base of the primary cilium, where it stabilizes the microtubule axoneme [36,37]. NEK1 has also been implicated in mitochondrial dynamics, particularly in fission and fusion processes, which are essential for maintaining mitochondrial integrity and cellular homeostasis. NEK1-deficient MEF cells display abnormal mitochondrial fragmentation, potentially linked to vacuolar protein sorting-associated protein 26B [38]. Mutations in NEK1 have been linked to several human diseases, including amyotrophic lateral sclerosis [39], in which mitochondrial dysfunction is a hallmark. Thus, NEK1′s involvement in mitochondrial function extends to its critical role in cellular health by modulating mitochondrial morphology, distribution, and stress response. Our study further reveals that NEK1 directly interacts with the mitochondrial protein MTFR1 to promote mitochondrial fusion, positioning NEK1 as a key regulator of mitochondrial homeostasis.

Conclusions

In summary, our study demonstrates that under low-glucose conditions, the interaction between NEK1 and MTFR1 is enhanced in colorectal cancer cells, leading to phosphorylation of MTFR1 at S119. This promotes mitochondrial fusion, maintains mitochondrial function, enhances oxidative phosphorylation, and supports cell survival in a low-glucose environment. Furthermore, MTFR1-S119 phosphorylation is crucial for colorectal cancer progression and may serve as a potential therapeutic target.

Funding

This research was supported by National Natural Science Foundation of China [82472860] and [82103198].

Data availability

All the raw data of this study are available from the corresponding author upon reasonable.

Ethics approval

The animal experiments conducted in this project were approved by the Animal Experimentation and Welfare Committee of Capital Medical University (AEEI-2024-255).

CRediT authorship contribution statement

Nan Zhang: Writing – original draft, Funding acquisition, Conceptualization. **Lu Dong:** Validation, Investigation. **Sifan Liu:** Validation, Investigation. **Tingting Ning:** Writing – review & editing, Supervision. **Shengtao Zhu:** Writing – review & editing, Funding acquisition.

Declaration of competing interest

The authors declare that they have no competing interests.

Supplementary materials

Supplementary material associated with this article can be found, in the online version, at doi:10.1016/j.neo.2025.101159.

References

[1] E. Morgan, M. Arnold, A. Gini, V. Lorenzoni, C.J. Cabasag, M. Laversanne, et al., Global burden of colorectal cancer in 2020 and 2040: incidence and mortality estimates from GLOBOCAN, Gut 72 (2) (2023) 338–344.
[2] Y-H Xie, Y-X Chen, J-Y. Fang, Comprehensive review of targeted therapy for colorectal cancer, Signal Transduct. Targeted Therapy 5 (1) (2020) 22.
[3] N. Hay, Reprogramming glucose metabolism in cancer: can it be exploited for cancer therapy? Nat. Rev. Cancer 16 (10) (2016) 635–649.
[4] B. Faubert, A. Solmonson, RJ. DeBerardinis, Metabolic reprogramming and cancer progression, Science 368 (6487) (2020).
[5] J. Zhu, CB. Thompson, Metabolic regulation of cell growth and proliferation, Nat. Rev. Mol. Cell Biol. 20 (7) (2019) 436–450.
[6] P.E. Porporato, N. Filigheddu, JMB-S Pedro, G. Kroemer, L. Galluzzi, Mitochondrial metabolism and cancer, Cell Res. 28 (3) (2018) 265–280.
[7] T. Wai, T. Langer, Mitochondrial Dynamics and Metabolic Regulation, Trends Endocrinol. Metab. 27 (2) (2016) 105–117.
[8] K. Wang, D.L. Zhang, B. Long, T. An, J. Zhang, L.Y. Zhou, et al., NFAT4-dependent miR-324-5p regulates mitochondrial morphology and cardiomyocyte cell death by targeting Mtfr1, Cell Death. Dis. 6 (12) (2015) e2007.
[9] M. Monticone, I. Panfoli, S. Ravera, R. Puglisi, M.M. Jiang, R. Morello, et al., The nuclear genes Mtfr1 and Dufd1 regulate mitochondrial dynamic and cellular respiration, J. Cell. Physiol. 225 (3) (2010) 767–776.
[10] NK, Evan Panchal, S. Prince, The NEK family of serine/threonine kinases as a biomarker for cancer, Clin. Exp. Med. 23 (1) (2023) 17–30.
[11] L.S. Reinhardt, A.M. Morás, J.G. Henn, P.R. Arantes, M.B. Ferro, E. Braganhol, et al., Nek1-inhibitor and temozolomide-loaded microfibers as a co-therapy strategy for glioblastoma treatment, Int. J. Pharm. 617 (2022) 121584.
[12] Y. Zhu, L. Gu, X. Lin, C. Liu, B. Lu, K. Cui, et al., Dynamic Regulation of ME1 Phosphorylation and Acetylation Affects Lipid Metabolism and Colorectal Tumorigenesis, Mol. Cell 77 (1) (2020) 138–149, e5.
[13] K. Qian, W. Li, S. Ren, W. Peng, B. Qing, X. Liu, et al., HDAC8 Enhances the Function of HIF-2α by Deacetylating ETS1 to Decrease the Sensitivity of TKIs in ccRCC, Adv Sci (Weinh) 11 (36) (2024) e2401142.
[14] M.B. Martins, A.M. Perez, V.A. Bohr, D.M. Wilson 3rd, J. Kobarg, NEK1 deficiency affects mitochondrial functions and the transcriptome of key DNA repair pathways, Mutagenesis 36 (3) (2021) 223–236.
[15] J. Li, Q. Huang, X. Long, X. Guo, X. Sun, X. Jin, et al., Mitochondrial elongation-mediated glucose metabolism reprogramming is essential for tumour cell survival during energy stress, Oncogene 36 (34) (2017) 4901–4912.
[16] S.J. Humphrey, D.E. James, M. Mann, Protein Phosphorylation: a major switch mechanism for metabolic regulation, Trends Endocrinol. Metab. 26 (12) (2015) 676–687.
[17] L. Ma, J. Wei, J. Wan, W. Wang, L. Wang, Y. Yuan, et al., Low glucose and metformin-induced apoptosis of human ovarian cancer cells is connected to ASK1 via mitochondrial and endoplasmic reticulum stress-associated pathways, J. Exp. Clin. Cancer Res. 38 (1) (2019) 77.
[18] A.V. Kuznetsov, S. Javadov, R. Margreiter, M. Grimm, J. Hagenbuchner, MJ. Ausserlechner, Structural and functional remodeling of mitochondria as an adaptive response to energy deprivation, Biochimica et Biophysica Acta (BBA) - Bioenergetics 1862 (6) (2021) 148393.
[19] K. Miki, M. Yagi, K. Yoshimoto, D. Kang, T. Uchiumi, Mitochondrial dysfunction and impaired growth of glioblastoma cell lines caused by antimicrobial agents inducing ferroptosis under glucose starvation, Oncogenesis 11 (1) (2022) 59.
[20] J.C. García-Cañaveras, L. Chen, JD. Rabinowitz, The Tumor Metabolic Microenvironment: Lessons from Lactate, Cancer Res. 79 (13) (2019) 3155–3162.
[21] M.V. Liberti, JW. Locasale, The warburg effect: how does it benefit cancer cells? Trends Biochem. Sci 41 (3) (2016) 211–218.
[22] R. Buono, VD. Longo, Starvation, Stress Resistance, and Cancer, Trends Endocrinol. Metab. 29 (4) (2018) 271–280.
[23] A.S. Rambold, B. Kostelecky, N. Elia, J. Lippincott-Schwartz, Tubular network formation protects mitochondria from autophagosomal degradation during nutrient starvation, P. Natl. Acad. Sci. USA 108 (25) (2011) 10190–10195.
[24] H. Guedouari, T. Daigle, L. Scorrano, E. Hebert-Chatelain, Sirtuin 5 protects mitochondria from fragmentation and degradation during starvation, Biochim. Biophys. Acta. Mol. Cell Res. 1864 (1) (2017) 169–176.
[25] S. Hasani, L.E.A. Young, W. Van Nort, M. Banerjee, D.R. Rivas, J. Kim, et al., Inhibition of mitochondrial fission activates glycogen synthesis to support cell survival in colon cancer, Cell Death. Dis. 14 (10) (2023) 664.
[26] J.Y. Lee, M. Kapur, M. Li, M.C. Choi, S. Choi, H.J. Kim, et al., MFN1 deacetylation activates adaptive mitochondrial fusion and protects metabolically challenged mitochondria, J. Cell Sci. 127 (Pt 22) (2014) 4954–4963.
[27] H. Zhang, Y. Zhao, Q. Yao, Z. Ye, A. Mañas, J. Xiang, Ubl4A is critical for mitochondrial fusion process under nutrient deprivation stress, PLoS One 15 (11) (2020) e0242700.
[28] C. Wu, W. Yao, W. Kai, W. Liu, W. Wang, S. Li, et al., Mitochondrial fusion machinery specifically involved in energy deprivation-induced autophagy, Front Cell Dev Biol. 8 (2020) 221.
[29] L. Tilokani, F.M. Russell, S. Hamilton, D.M. Virga, M. Segawa, V. Paupe, et al., AMPK-dependent phosphorylation of MTFR1L regulates mitochondrial morphology, Sci. Adv. 8 (45) (2022) eabo7956.
[30] L. Zhang, X. Zhang, H. Liu, C. Yang, J. Yu, W. Zhao, et al., MTFR2-dependent mitochondrial fission promotes HCC progression, J. Transl. Med. 22 (1) (2024) 73.
[31] W. Wang, M. Xiong, L. Jiang, Z. Chen, Y. Shao, MTFR2 Promotes the Proliferation, Migration, and Invasion of Oral Squamous Carcinoma by Switching OXPHOS to Glycolysis, Front. Oncol. 10 (2020) 858.
[32] A. Peres de Oliveira, L. Kazuo Issayama, I.C. Betim Pavan, F. Riback Silva, T. Diniz Melo-Hanchuk, F. Moreira Simabuco, et al., Checking NEKs: overcoming a bottleneck in human diseases, Molecules 25 (8) (2020) 1778.
[33] A.M. Fry, L. O'Regan, S.R. Sabir, R. Bayliss, Cell cycle regulation by the NEK family of protein kinases, J. Cell Sci. 125 (Pt 19) (2012) 4423–4433.
[34] A.L. Pelegrini, D.J. Moura, B.L. Brenner, P.F. Ledur, G.P. Maques, J.A. Henriques, et al., Nek1 silencing slows down DNA repair and blocks DNA damage-induced cell cycle arrest, Mutagenesis 25 (5) (2010) 447–454.
[35] O. Shalom, N. Shalva, Y. Altschuler, B. Motro, The mammalian Nek1 kinase is involved in primary cilium formation, FEBS Lett. 582 (10) (2008) 1465–1470.
[36] W. Wang, T. Wu, MW. Kirschner, The master cell cycle regulator APC-Cdc20 regulates ciliary length and disassembly of the primary cilium, eLife 3 (2014) e03083.
[37] C. Thiel, K. Kessler, A. Giessl, A. Dimmler, S.A. Shalev, S. von der Haar, et al., NEK1 mutations cause short-rib polydactyly syndrome type majewski, Am. J. Hum. Genet. 88 (1) (2011) 106–114.
[38] H. Wang, W. Qi, C. Zou, Z. Xie, M. Zhang, M.G. Naito, et al., NEK1-mediated retromer trafficking promotes blood-brain barrier integrity by regulating glucose metabolism and RIPK1 activation, Nat. Commun. 12 (1) (2021) 4826.
[39] J.R. Mann, E.D. McKenna, D. Mawrie, V. Papakis, F. Alessandrini, E.N. Anderson, et al., Loss of function of the ALS-associated NEK1 kinase disrupts microtubule homeostasis and nuclear import, Sci. Adv. 9 (33) (2023) eadi5548.